



Biomechanical comparison of multi-rod constructs by satellite rod configurations (in-line vs. lateral) and screw types (monoaxial vs. polyaxial) spanning a lumbar pedicle subtraction osteotomy (PSO): is there an optimal configuration?

Niloufar Shekouhi¹ · Ardalan S. Vosoughi¹ · Joseph M. Zavatsky² · Vijay K. Goel¹ · Alekos A. Theologis³

Received: 19 October 2021 / Revised: 10 April 2022 / Accepted: 20 July 2022 / Published online: 6 August 2022
© The Author(s) 2022

Abstract

Purpose Multi-rod constructs are used commonly to stabilize pedicle subtraction osteotomies (PSO). This study aimed to evaluate biomechanical properties of different satellite rod configurations and effects of screw-type spanning a PSO.

Methods A validated 3D spinopelvic finite element model with a L3 PSO (30°) was used to evaluate 5 models: (1) Control (T10–pelvis + 2 rods); (2) lateral satellite rods connected via offsets to monoaxial screws (LatSat-Mono) or (3) polyaxial screws (LatSat-Poly); (4) in-line satellite rods connected to monoaxial screws (InSat-Mono) or (4) polyaxial screws (InSat-Poly). Global and PSO range of motions (ROM) were recorded. Rods' von Mises stresses and PSO forces were recorded and the percent differences from Control were calculated.

Results All satellite rods (save InSat-Mono) increased PSO ROM and decreased primary rods' von Mises stresses at the PSO. Lateral rods increased PSO forces (LatSat-Mono: 347.1 N; LatSat-Poly: 348.6 N; Control: 336 N) and had relatively lower stresses, while in-line rods decreased PSO forces (InSat-Mono: 280.1 N; InSat-Poly: 330.7 N) and had relatively higher stresses. Relative to polyaxial screws, monoaxial screws further decreased PSO ROM, increased satellite rods' stresses, and decreased PSO forces for in-line rods, but did not change PSO forces for lateral rods.

Conclusion Multi-rod constructs using in-line and lateral satellite rods across a PSO reduced primary rods' stresses. Subtle differences in biomechanics suggest lateral satellite rods, irrespective of screw type, increase PSO forces and lower rod stresses compared to in-line satellite rods, which had a high degree of posterior instrumentation stress shielding and lower PSO forces. Clinical studies are warranted to determine if these findings influence clinical outcomes.

Keywords Finite element analysis · Pedicle subtraction osteotomy · Rod fracture · Pseudarthrosis · Multi-rod construct

Introduction

Lumbar pedicle subtraction osteotomies (PSO) are powerful surgical techniques to correct rigid and severe coronal and sagittal spinal malalignment. While providing significant

correction, they are associated with a relatively high rate of short- and long-term complications [1, 2]. Two of importance are pseudarthrosis and rod breakage, which have been reported as the most common postoperative complications and frequent indications for revision operations [2–11]. In an attempt to decrease their rates, a variety of supplementary surgical techniques have been evaluated and implemented. These have included multi-rod constructs stabilizing the PSO, interbody cages adjacent to the PSO, and varying rod materials and diameters spanning the PSO [4, 10, 12–17].

Multi-rod constructs can be achieved using either “satellite” rods (rods not connected to the primary rods) and/or “accessory rods” (rods connected to the primary rods) [18]. The first report of a multi-rod construct across a PSO was by Gupta et al. [4] who utilized a laterally based satellite rod

✉ Alekos A. Theologis
alekos.theologis@ucsf.edu

¹ Engineering Center for Orthopedic Research Excellence (E-CORE), Departments of Bioengineering and Orthopaedic Surgery, University of Toledo, Toledo, OH, USA

² Spine & Scoliosis Specialists, Tampa, FL, USA

³ Department of Orthopedic Surgery, University of California - San Francisco (UCSF), 500 Parnassus Ave, MUW 3rd Floor, San Francisco, CA 94143, USA

connected to a posted pedicle screw system (i.e., monoaxial screws that connect to rods via slotted connectors, which are secured to the screw shaft via a locking nut) above and below the PSO. Lateral satellite rods can be particularly useful from a surgical perspective, as they provide temporary stabilization while the PSO is being performed, facilitate closure of the osteotomy site (symmetric and/or asymmetric), and serve as the final fixation rods across the PSO without needing to be exchanged. As posted screw systems are now antiquated, the senior author has adapted the laterally based satellite rod technique of Gupta et al. using modern polyaxial screw systems by connecting a rod laterally to the screws above and below the PSO site via lateral offset connectors (Fig. 1).

As lateral satellite rod constructs have yet to be studied biomechanically and prior multi-rod biomechanical analyses have only focused on in-line satellite rods (Fig. 1) and accessory rods, the purpose of this study is to evaluate the biomechanical properties of in-line vs. laterally based satellite rods with different screw types (monoaxial vs. polyaxial) adjacent to a lumbar PSO site.

Methods

A previously validated three-dimensional osseoligamentous spinopelvic finite element model (T10–pelvis) with a 30° PSO at L3 was used [15]. The intact model was reconstructed from computed tomography (CT) scans of a human spine using MIMICS (Materialize Inc., Leuven, Belgium) software. IAFE-MESH (University of Iowa, Iowa) and HyperMesh (Altair Engineering, Michigan, USA) were used to create hexahedral elements (C3D8) of the vertebrae and tetrahedral elements (C3D4) of the pelvis. The meshed components were assembled in the Abaqus 6.14 (Dassault

Systems, Simile Inc., Providence, RI, USA). The spinal and sacroiliac ligaments were modeled using truss elements. In the vertebral body, a layer of 0.5 mm cortical bone was simulated to surround the cancellous bone [15, 19].

The intervertebral disks were composed of annulus fibrosis and nucleus pulposus. The annulus fibrosis was simulated using a solid ground substance (C3D8 elements) reinforced with rebar elements (embedded with $\pm 30^\circ$ angles). The nucleus pulposus was modeled using C3D8 elements with hyper-elastic Mooney–Rivlin formulation [15, 20]. The sacroiliac joint was modeled using soft contact with exponential behavior [15, 21]. Material properties were assigned to each component based on the literature (Table 1) [15].

The PSO model utilized in this study was previously performed and validated [15]. The anterior section was tied, while at the posterior, a surface-to-surface interaction (friction=0.46) was defined between the two resected segments [15].

The instrumentation including rods, pedicle screws, and lateral connectors was designed in SolidWorks (Dassault Systems, SolidWorks Corporation, Waltham, MA, USA) and imported into Abaqus for model development. Each pedicle screw was modeled in two parts (tulip and shaft) connected with a ball and socket joint. The pedicles at T10, T11, and T12 were instrumented with 6.5×40 mm polyaxial screws. At L1 and L5, 6.5×45 mm polyaxial screws were used. Adjacent to the osteotomy site (L2 and L4), 6.5×40 mm screws were inserted. The S1 pedicles and iliac screws were sized 7.5×50 mm and 8.5×80 mm polyaxial screws, respectively. In the “Control” model, two bilateral 5.5 mm cobalt–chromium rods were connected all screw tulips from T10 to the pelvis. In all of the other 4 constructs (multi-rod; see below), primary rods were connected to the screws’ tulips from T10 to ilium, except at L2 and L4 where the satellite rods were connected.

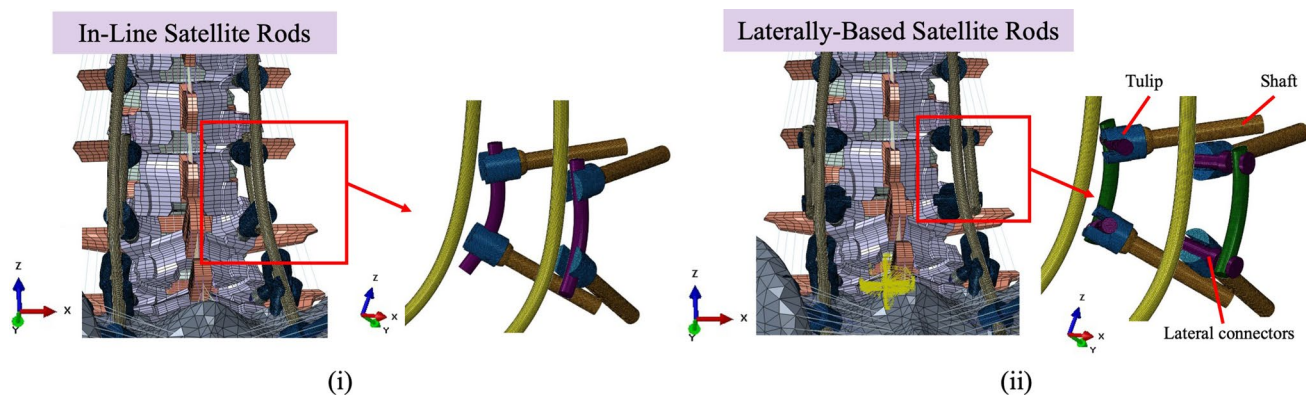


Fig. 1 Various rod and screw configurations simulated in this study to stabilize a L3 PSO. The model with two primary rods from T10–pelvis (Control) was modified to accommodate (i) in-line satellite rods connected to monoaxial screws (InSat-Mono) and polyaxial screws

(InSat-Poly) and (ii) laterally based satellite rods connected to monoaxial screws (LatSat-Mono) and polyaxial screws (LatSat-Poly) via offset attachments. Screw types refer to those above and below PSO site

Table 1 Material properties used in model development adapted from literature [15]

| Components | Element formulation | Young's modulus (MPa)/Poisson's ratio |
|---------------------------|---|---------------------------------------|
| Vertebral cortical bone | Isotropic, elastic hex elements (C3D8) | 12,000/0.3 |
| Vertebral cancellous bone | Isotropic, elastic hex elements (C3D8) | 100/0.2 |
| Pelvic cortical bone | Isotropic, elastic hex elements (C3D8) | 17,000/0.3 |
| Pelvic cancellous bone | Isotropic, elastic hex elements (C3D8) | 10/0.2 |
| Annulus (ground) | Neo-Hookean, hex elements (C3D8) | $C1=0.348, D1=0.3$ |
| Annulus (fiber) | Rebar | 357–550 |
| Nucleus | Mooney Rivlin hex elements (C3D8H) | $C1=0.12, C2=0.03, D1=0.0005$ |
| Apophyseal joints | Nonlinear soft contact, GAPUNI elements | – |
| Sacroiliac joints | Nonlinear soft contact | – |
| Ligaments | Hypo-elastic, tension only, Truss elements (T3D2) | Nonlinear stress–strain curves |
| Ti6Al4V pedicle screws | Isotropic, tetrahedron elements (C3D4) | 11,500/0.3 |
| CoCr rods | Isotropic, tetrahedron elements (C3D4) | 241,000/0.3 |

The following instrumentation configurations were simulated and compared:

- (a) Control: Primary rods (one on each side of spine) from T10–pelvis with polyaxial screws (Fig. 2a).
- (b) InSat-Poly: In-line satellite rods connected to polyaxial screws above and below the PSO site (Figs. 1 and 2b).

- (c) InSat-Mono: In-line satellite rods connected to monoaxial screws above and below the PSO site (Figs. 1 and 2b).
- (d) LatSat-Poly: Lateral satellite rods connected to polyaxial screws via offset lateral connectors above and below the PSO site (Figs. 1 and 2c).

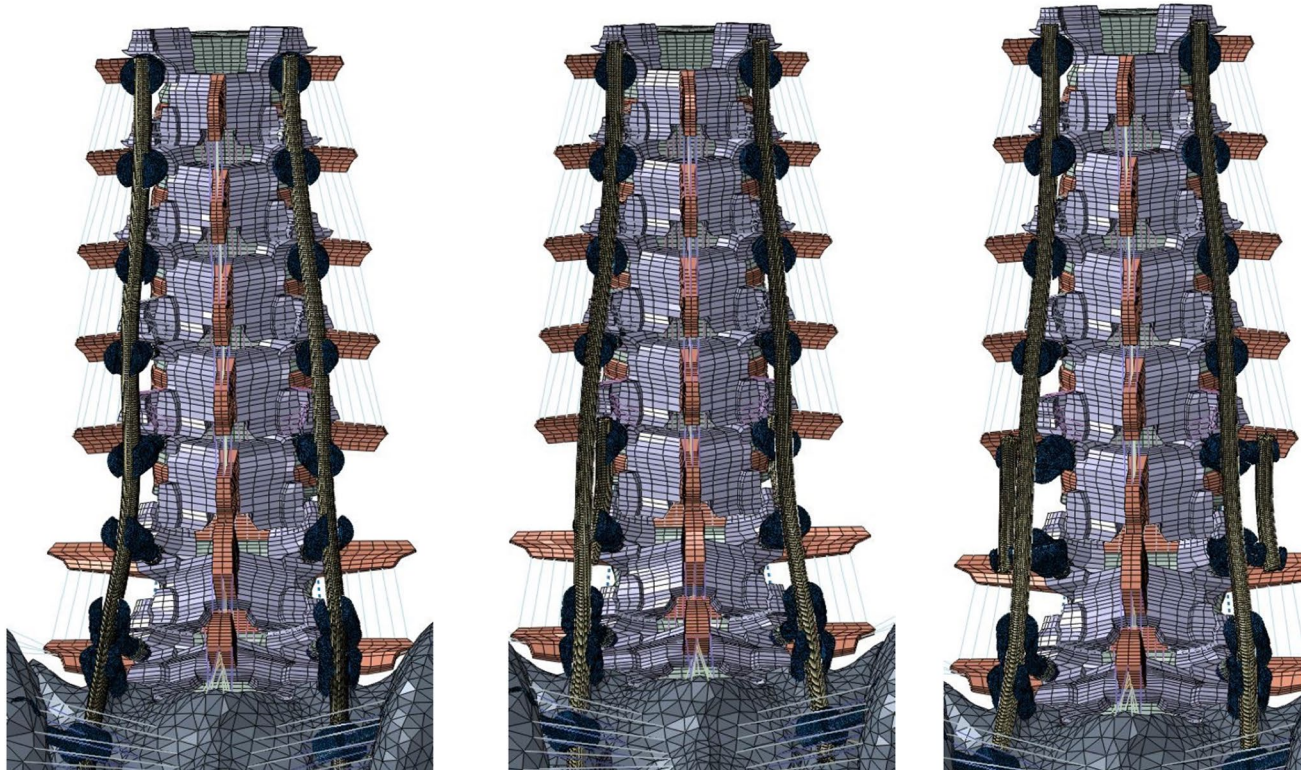


Fig. 2 Posterior view of various instrumentation configurations following lumbar PSO. Left panel: instrumented PSO model with two primary rods (Control). Middle panel: four-rod instrumented model

supplemented with in-line satellite rods (InSat-Mono and InSat-Poly). Right panel: four-rod instrumented model supplemented with laterally based satellite rods (LatSat-Mono and LatSat-Poly)

(e) LatSat-Mono: Lateral satellite rods connected to mono-axial screws via offset lateral connectors above and below the PSO site (Figs. 1 and 2c).

FE model development

The mesh convergence study was performed in two steps. First, a three-point bending simulation was performed on a single screw shaft and seed sizes were reduced until the difference between the yield loads obtained from two subsequent seed sizes was less than 5%. Second, the LatSat-Mono model was used to perform the mesh convergence study on the rods. Seed sizes were reduced until the percentage difference between the forces across the PSO site was below 5%.

In all levels except the PSO site, the shaft and tulip components were assembled and inserted under the guidance of spine surgeons. To accommodate the primary rods over the satellite rods, the primary rods were bent less than the satellite rods and the screws above and below the PSO site (i.e., L3 and L5) were recessed deeper than the other screws (i.e., T10, T11, T12, L1, L2, and S1). To keep the curvature of the rods similar in models with mono- and polyaxial screws the screw shafts were aligned with the tulip heads at the PSO site. Different interactions were defined between the screw shaft and the tulip head; in models with monoaxial screws, the tulip head was tied to the shaft. To simulate polyaxial screws, the same procedure was used as literature [22]. First, two reference points were defined on the screw shaft and the tulip head and the corresponding nodes were coupled to each reference point. Then, a “Join-Cardan” connector was assigned between the shaft & tulip which constrained the two components in U1, U2, and U3 motions and allows for a relative rotation between these components (UR1, UR2, and UR3). Moreover, a surface-to-surface interaction was defined between the tulip and shaft (friction = 0.4 [23]). Rods were tied to tulip and lateral connectors.

A two-step analysis was performed. In step 1, follower loads were applied using wire elements (with axial connector type) which followed the curvature of the thoracolumbar segments. A 300 N connector load was applied to the thoracic (150 N to left and right side) and a 400 N connector load was applied to the lumbar spine (200 N to left and right side). Additionally, a concentrated force with the magnitude of 400 N was applied to the sacrum to account for the body weight and muscle forces [15]. In step 2, pure moments of 7.5 Nm were applied to the top endplate of the T10 vertebra in all anatomical directions. In both steps, the acetabulum surfaces of the pelvis were fixed in all degrees of freedom.

Data analysis

For each configuration, the range of motions (ROM) of T10–S1 (global) and L2–L4 (PSO) were recorded at the

second step. The von Mises stresses on the primary/satellite rods were recorded and the percentage differences to the primary rods in the Control model were calculated. Due to the complexity in loading and geometry of the lumbar spine PSO model, von Mises stresses, instead of individual components of stress, were used as von Mises stress is a commonly used criterion for yielding or fracture under complex loading. The critical stress locations were recorded and compared among all models. For each model, the force acting at the osteotomy site in flexion motion was captured.

Results

T10–S1/global range of motion

Data on T10–S1 ROM are presented in Fig. 3. Use of satellite rods in any configuration (in-line and lateral) decreased T10–S1 ROM in flexion–extension and lateral bending [15]. Lateral satellite rods decreased global ROM flexion [LatSat-Poly: 8% (3.16 degrees); LatSat-Mono: 9% (3.15 degrees)] and extension [LatSat-Poly: 37% (0.62 degrees); LatSat-Mono: 39% (0.6 degrees)] compared to the Control (flexion: 3.45 degrees; extensions: 0.99 degrees). In-line satellite rods decreased global ROM flexion [InSat-Poly: 11% (3.08 degrees); InSat-Mono: 38% (2.97 degrees)] and extension [InSat-Poly: 14% (0.61 degrees); InSat-Mono: 47% (0.52 degrees)] compared to the Control (flexion: 3.45 degrees; extensions: 0.99 degrees). All four multi-rod configurations showed approximately similar ROM in lateral bending. Global ROM in axial rotation increased for lateral satellite rods (LatSat-Poly: 3.38–3.5 degrees; LatSat-Mono: 3.34–3.44 degrees) and in-line satellite rods (InSat-Poly: 3.35–3.4 degrees; InSat-Mono: 3.34–3.43 degrees) compared to the Control (2.86–3.01 degrees).

L2–L4 (PSO) Range of Motion

Data on L2–4 ROM (across the L3 PSO site) are presented in Fig. 4. Lateral satellite rods increased L2–L4 ROM in flexion [LatSat-Poly: 38% (1.16 degrees); LatSat-Mono: 19% (1.0 degrees)] and extension [LatSat-Poly: 315% (0.64 degrees); LatSat-Mono: 212% (0.48 degrees)] compared to Control (flexion: 0.84, extension: 0.15 degrees). Note that use of mono-axial screws resulted in lower L2–4 ROM compared to polyaxial screws. For in-line satellite rods, use of polyaxial screws (InSat-Poly) increased PSO flexion by 22% (1.03 degrees) and extension 278% (0.58 degrees), while use of monoaxial screws (InSat-Mono) decreased PSO ROM in flexion by 18% (0.69 degrees) and increased the ROM in extension 107% (0.32 degrees) compared to the Control. Moreover, in-line satellite rods had lower PSO ROM compared to lateral satellite rod configurations in lateral bending and axial rotation.

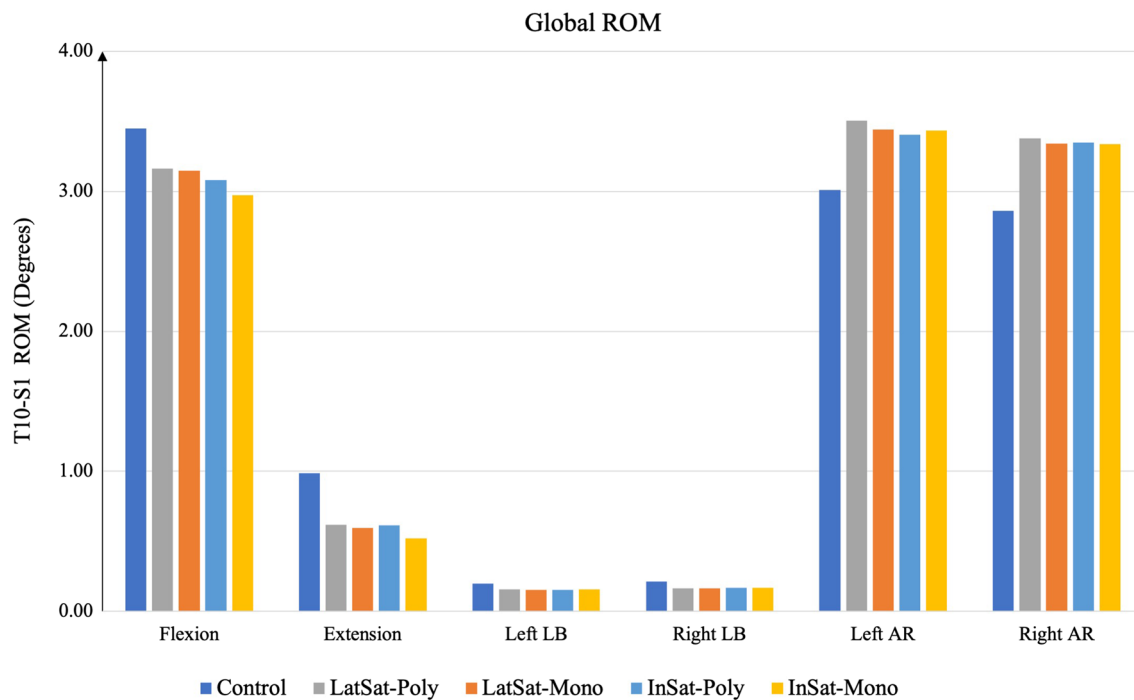


Fig. 3 T10–S1 range of motion for: two primary rods connected to polyaxial screws (Control), laterally based satellite rods connected to polyaxial screws (LatSat-Poly), laterally based satellite rods connected to monoaxial screws (LatSat-Mono), satellite rods connected

to polyaxial screws (InSat-Poly), and satellite rods connected to monoaxial screws (InSat-Mono). Using satellite rods decreased the global ROM compared to two-rod configuration in flexion–extension and lateral bending, however, it increased the ROM in axial rotation

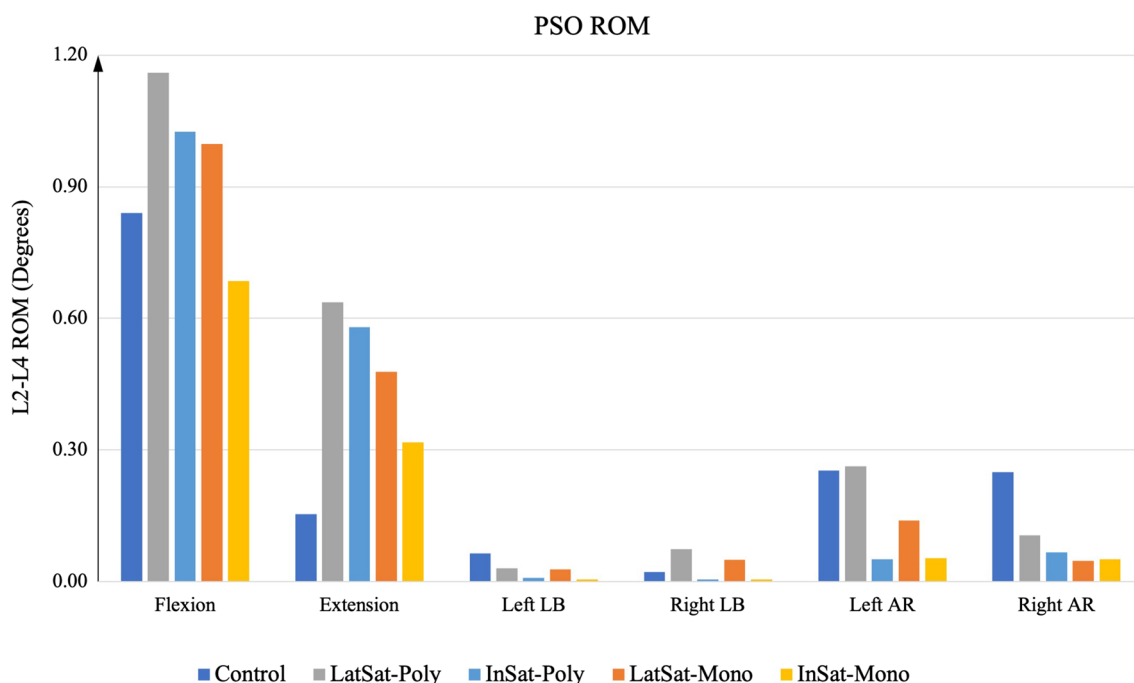


Fig. 4 L2–L4 range of motion for two primary rods connected to polyaxial screws (Control), laterally based satellite rods connected to polyaxial screws (LatSat-Poly), laterally based satellite rods connected

to monoaxial screws (LatSat-Mono), satellite rods connected to polyaxial screws (InSat-Poly), and satellite rods connected to monoaxial screws (InSat-Mono)

von Mises stresses

Data on maximal von Mises stresses on the posterior rods, primary and satellite, are presented in Table 2 and Fig. 5. Compared to in-line configurations, lateral rods decreased stresses on primary rods to a similar extent, but had considerably lower stresses themselves. Compared to the Control

model, reduction in primary rods' von Mises stresses was similar between lateral and in-line configurations. Satellite rods provided greatest percent reduction in von Mises stresses on primary rods during flexion and lateral bending. Lateral satellite rods' von Mises stresses were considerably less than the von Mises stresses on in-line satellite rods. For all satellite rods, von Mises stresses were greatest during

Table 2 Values of maximum von Mises stress (MPa) for the Control construct

| | Rod | Control | LatSat-Mono | LatSat-Poly | InSat-Mono | InSat-Poly |
|-----------|-----------|---------|-----------------|-----------------|-----------------|----------------|
| Flexion | Primary | 294.4 | 203 (– 31%) | 205.3 (– 30.2%) | 183 (– 37.8%) | 189 (– 35.8%) |
| | Satellite | n/a | 85.8 | 37 | 207 | 117 |
| Extension | Primary | 84.4 | 75.06 (– 11%) | 75 (– 11.13%) | 95.5 (13.15%) | 74.7 (– 11.5%) |
| | Satellite | n/a | 45 | 25 | 91 | 43.4 |
| Left LB | Primary | 216.4 | 164.8 (– 23.8%) | 163 (– 24.6%) | 170 (– 21.4%) | 172 (– 20.5%) |
| | Satellite | n/a | 63.5 | 24.2 | 136.2 | 82.8 |
| Right LB | Primary | 217.9 | 152.6 (– 29.9%) | 153 (– 29.9%) | 157 (– 27.9%) | 145.9 (– 33%) |
| | Satellite | n/a | 72 | 25.7 | 148 | 81.17 |
| Left AR | Primary | 258.5 | 225 (– 12.9%) | 208 (– 19.5%) | 192.4 (– 25.5%) | 205 (– 20.7%) |
| | Satellite | n/a | 86 | 30.1 | 134.6 | 79 |
| Right AR | Primary | 229 | 205.3 (– 10.3%) | 211.5 (– 7.6%) | 205.6 (– 10.2%) | 207 (– 9.6%) |
| | Satellite | n/a | 63.7 | 39 | 134.7 | 71.4 |

For all other models, percent differences between stresses on the primary and satellite rods from the Control model were reported

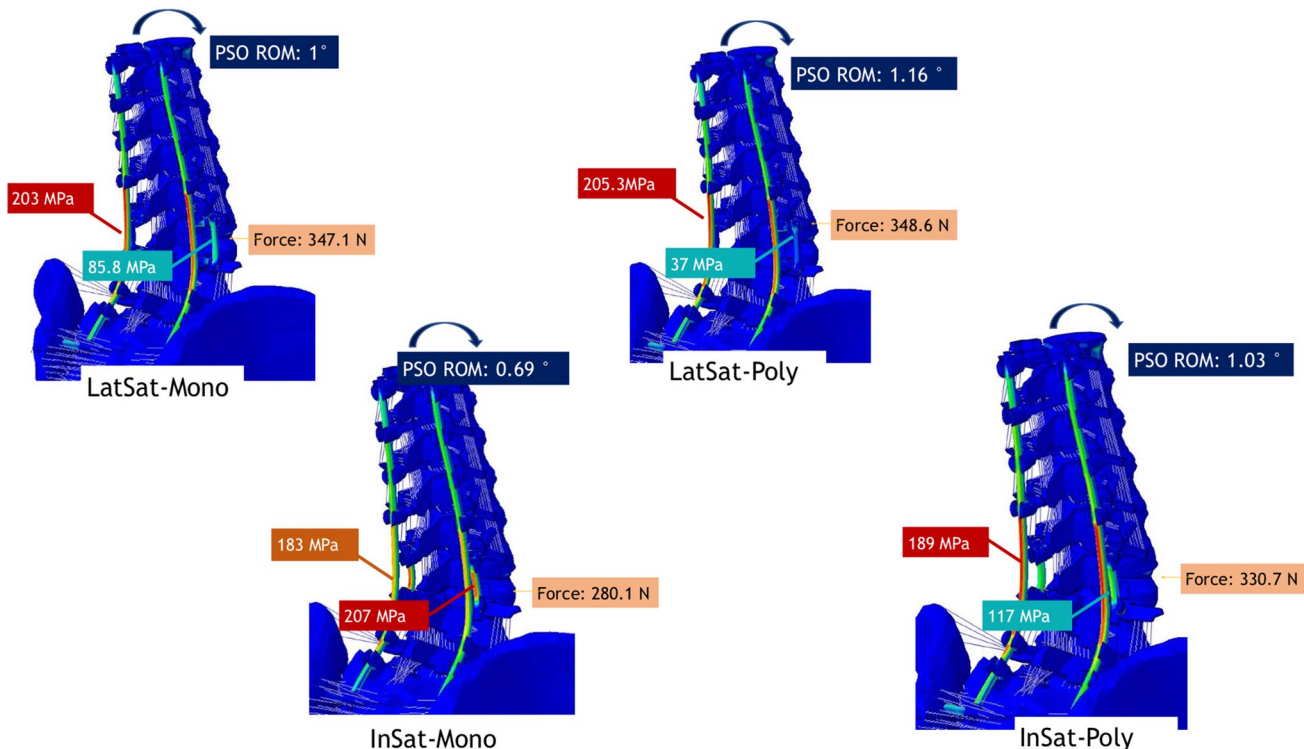


Fig. 5 Visual comparison of the four-rod techniques presented in this study. Models include laterally based satellite rods connected to polyaxial screws (LatSat-Poly), laterally based satellite rods connected to

monoaxial screws (LatSat-Mono), in-line satellite rods connected to polyaxial screws (InSat-Poly), and in-line satellite rods connected to monoaxial screws (InSat-Mono)

flexion and lowest during extension. Of note, InSat-Mono was the only construct to demonstrate an increase in stresses on the primary rods in extension (+13.15%) compared to the Control (Table 2). Also, the data demonstrated that polyaxial screws at the osteotomy site (LatSat-Poly & InSat-Poly) resulted in lower stresses on satellite rods compared to models with monoaxial screws for both lateral and in-line configurations (Table 2).

In the four-rod configurations, two critical stress locations were observed: adjacent to the PSO site and at the L5–S1 level. The critical stress location was observed on primary rods for all multi-rod constructs at the PSO site except during lateral bending and extension where the maximal stresses were adjacent to L5–S1. Additionally, the InSat-Mono model showed slightly higher stresses on the satellite rods than the primary rods.

Force at the PSO site (Table 3)

Data on forces at the PSO site are presented in Table 3. Compared to the Control, lateral satellite rods increased the force across the osteotomy site. In contrast, in-line satellite rods (most notably InSat-Mono) showed lower PSO forces than the Control construct. While screw types above and below the PSO did not result in a difference in PSO forces for lateral satellite rods, monoaxial screws with in-line rods (InSat-Mono) had 50 N lower PSO forces than polyaxial screws with in-line rods (InSat-Poly).

Discussion

Multiple prior studies have evaluated the relative biomechanical behaviors of in-line satellite rods and accessory rods, but none have evaluated the biomechanics of lateral satellite rod constructs across a lumbar PSO. As such, the

Table 3 The forces across the osteotomy site under flexion for different configurations simulated in this study

| | |
|-------------|-----------|
| Control | 336 (N) |
| LatSat-Mono | 347.1 (N) |
| LatSat-Poly | 348.6 (N) |
| InSat-Mono | 280.1 (N) |
| InSat-Poly | 330.7 (N) |

Using laterally based satellite rods increased the PSO force while the in-line satellite rods decreased the force at the osteotomy site compared to the Control model

Control: two primary rods connected to polyaxial screws, *LatSat-Poly:* laterally based satellite rods connected to polyaxial screws, *LatSat-Mono:* laterally based satellite rods connected to monoaxial screws, *InSat-Poly:* satellite rods connected to polyaxial screws, *InSat-Mono:* satellite rods connected to monoaxial screws

study presented herein investigated the relative biomechanical effects of lateral versus in-line satellite rods with different screw types (monoaxial vs. polyaxial) adjacent to a lumbar PSO site using a well-accepted validated FE model for long thoracolumbar spine instrumentations. These results are consistent with prior reports, but also add unique information to the literature on biomechanics of multi-rod constructs for lumbar PSOs, particularly lateral satellite rods.

Our FE predictions showed that using satellite rods (in-line and lateral) reduced von Mises stresses on primary rods at the PSO compared to the Control model, which is in agreement with prior reports [9, 12–14, 24–27]. This benefit appears to be in part secondary to allowing primary rods to be undercontoured at the PSO site. Gupta et al. reported that when the osteotomy site is closed by satellite rods independent from the primary rods, a sharp curvature at the apex of the primary rods is avoided, which eventually will lead to less primary rod stresses and theoretically lower rates of rod breakage [4]. This was demonstrated by Gelb et al. who found that in-line satellite rods across a PSO decreased primary rod stresses, as the satellite rods allowed the primary rods to be undercontoured by 14.2° [17, 28]. As the vast majority of rod fractures occur at the level of the PSO [6], this effect of satellite rods on reducing primary rod stresses is important.

Lateral and in-line satellite rod configurations' reduction on primary rod stresses appears to be a result of different biomechanical effects on the PSO site. We found that lateral satellite rods increased PSO ROM in flexion and extension, which resulted in less von Mises stress on the lateral satellite rods and increased force at the PSO site. This is in contrast to in-line satellite rods, which resulted in decreased force at the PSO likely as a consequence of the in-line rods creating a relatively stiffer construct across the PSO site (less PSO ROM relative to the lateral satellite rods, particularly with monoaxial screws). This relative increased stiffness transferred the forces and stress from the PSO site to the in-line satellite rods, as evidenced by the considerably higher von Mises stresses observed on the in-line satellite rods themselves. These data suggest that the lateral satellite rods, irrespective of screw type, create a better biomechanical environment across the PSO site compared to in-line satellite rods, as the forces are transferred away from the lateral and primary rods and to the anterior vertebral column [11]. This is postulated to be biomechanically favorable for the PSO site, as increased PSO forces should promote bone-healing and fusion at the osteotomy site and decrease the chances of non-union compared to the in-line configurations, a theory also supported by La Barbera et al. [11]. This currently is purely a theory, and has yet to be proven. As such, it deserves further investigation. Note that ROM from T10 to S1 is

not altered appreciably by any satellite rod configuration, which is likely secondary to the fact that the control and the four satellite rod configurations all include rods that stabilize the spine from T10 to the pelvis and that the satellite rods only span 2 levels (L3–L5).

Our results on the effects of screw type (monoaxial vs. polyaxial) used to stabilize satellite rods across the PSO provide an added dimension to the discussion in the prior paragraph. Consistently, monoaxial screws in this study created a stiffer PSO site relative to polyaxial screws, as evidenced by decreased PSO ROM in all directions for both types of satellite rods. This relative decreased ROM afforded by monoaxial screws was subsequently manifested in higher von Mises stresses on satellite rods for both types of satellite rods. While this stress shielding by the posterior instrumentation resulted in significantly lower PSO forces for in-line satellite rods with monoaxial screws (56 N less than controls) compared to in-line rods with polyaxial screws (5 N less than controls), there was no difference in forces across the PSO site for lateral satellite rods with monoaxial screws compared to lateral rods with polyaxial screws. In fact, the lateral satellite rods with monoaxial screws resulted in an increase in PSO forces, the values of which were similar to lateral satellite rods with polyaxial screws. Given the anterior load sharing afforded by the lateral satellite rod constructs, they appear to offer superior biomechanical PSO environments relative to in-line satellite rod configurations. These data suggest that LatSat-Mono may offer the best biomechanical PSO environment, while the InSat-Mono creates the most unfavorable biomechanical PSO environment.

The results of this study should be considered in the context of its limitations. These include the lack of range of motion data for the cadaveric spine with lateral satellite rod configurations, simulation performed with no muscle forces, and using uncomplicated geometries of the implants and simplified contact and constraints. Moreover, the residual stresses produced as a result of rod contouring and screw/rod tightening were not considered. Specifically, the interconnections of the screws, rods, lateral connectors, and anatomy were all in ideal conditions, which is almost never the case clinically. The lack of motion between the lateral satellite rods and the connectors may have stiffened the lateral satellite rods making them appear better when in practice those interconnections may create a less stiff construct over the PSO. As such, future investigations should ideally incorporate movement between the rod and connector or screw and connector. Our finding that satellite rods affect more than just reducing ROM across the PSO in flexion deserves further scrutiny. It may imply that the moment is not about the instantaneous axis of rotation of the PSO and perhaps posterior to it, which may or may not be physiologic. Alternatively, satellite rods' effects on biomechanics may also be influenced by other factors, including rod characteristics

(i.e., diameter, material, bend magnitude). Additionally, as utilization of laterally based satellite rods is relatively new for PSO closure and stabilization, we are unable to comment upon the clinical significance of our observed biomechanical differences and relative long-term clinical performance of the different instrumentation configurations evaluated in this study. Of note, however, all techniques have been performed safely and without any notable clinical differences in the short-term. Despite these limitations, the advantageous biomechanical data of laterally based satellite rods observed in our study are noteworthy when considered in the context of the purported benefits imparted by lateral satellite rods on the surgical workflow while performing a lumbar PSO [i.e., providing temporary stabilization while the PSO is being performed, facilitating closure of the osteotomy site (symmetric and/or asymmetric), and serving as the final fixation rods across the PSO without needing to be exchanged].

Conclusion

In this FE analysis of a L3 PSO, multi-rod constructs using in-line and lateral satellite rods reduced stresses on primary rods at the PSO site. This was afforded by different relative distributions of forces and stresses on the PSO site and satellite rods between the two satellite rod configurations. Specifically, lateral satellite rods distributed forces more advantageously (increased PSO forces and low von Mises stresses on the satellite rods—low degree of stress shielding on posterior instrumentation) compared to in-line satellite rods (decreased PSO forces and high von Mises stresses on the satellite rods—high degree of stress shielding on posterior instrumentation). Monoaxial screws created a particularly favorable biomechanical PSO environment when combined with lateral satellite rods, but unfavorable biomechanical conditions when combined with in-line satellite rods. As the biomechanics differences observed between the constructs in this study are subtle, these data deserve further attention through additional in vitro and clinical studies.

Authors' contributions All authors made substantial contributions to the conception or design of the work, the acquisition, analysis, or interpretation of data, drafted the work or revised it critically for important intellectual content, approved the version to be published, and agree to be accountable for all aspects of the work in ensuring that questions related to the accuracy or integrity of any part of the work are appropriately investigated and resolved.

Funding The work was supported in part by NSF Industry/University Cooperative Research Center at UCSF, The University of Toledo, and The Ohio State University (www.nsfcdmi.org).

Availability of data and materials All data generated or analyzed during this study are included in this published article.

Code availability No software application or custom code was utilized.

Declarations

Conflicts of interest The authors have no conflicts of interest to declare that are relevant to the content of this article.

Ethics approval As the study involved no patient or clinical data, no ethical approval was required.

Consent to participate As the study involved no patient or clinical data, consent to participate was not required.

Consent for publication As the study involved no patient or clinical data, consent for publication was not required.

Open Access This article is licensed under a Creative Commons Attribution 4.0 International License, which permits use, sharing, adaptation, distribution and reproduction in any medium or format, as long as you give appropriate credit to the original author(s) and the source, provide a link to the Creative Commons licence, and indicate if changes were made. The images or other third party material in this article are included in the article's Creative Commons licence, unless indicated otherwise in a credit line to the material. If material is not included in the article's Creative Commons licence and your intended use is not permitted by statutory regulation or exceeds the permitted use, you will need to obtain permission directly from the copyright holder. To view a copy of this licence, visit <http://creativecommons.org/licenses/by/4.0/>.

References

1. Daubs MD, Brodke DS, Annis P, Lawrence BD (2016) Perioperative complications of pedicle subtraction osteotomy. *Glob Spine J* 6:630–635
2. Annis P, Dheerendra S, Daubs M, Brodke D (2016) Perioperative complications of pedicle subtraction osteotomy. *Spine J* 16:S67
3. Smith JS, Shaffrey CI, Klineberg E, Lafage V, Schwab F, Lafage R, Kim HJ, Hostin R, Mundis GM, Gupta M (2017) Complication rates associated with 3-column osteotomy in 82 adult spinal deformity patients: retrospective review of a prospectively collected multicenter consecutive series with 2-year follow-up. *J Neurosurg Spine* 27:444–457
4. Gupta S, Eksi MS, Ames CP, Deviren V, Durbin-Johnson B, Smith JS, Gupta MC (2018) A novel 4-rod technique offers potential to reduce rod breakage and pseudarthrosis in pedicle subtraction osteotomies for adult spinal deformity correction. *Oper Neurosurg (Hagerstown)* 14:449–456. <https://doi.org/10.1093/ons/oxp151>
5. Smith JS, Shaffrey CI, Ames CP, Demakakos J, Fu K-MG, Kesavarasi S, Li CM, Deviren V, Schwab FJ, Lafage V (2012) Assessment of symptomatic rod fracture after posterior instrumented fusion for adult spinal deformity. *Neurosurgery* 71:862–868
6. Smith JS, Shaffrey E, Klineberg E, Shaffrey CI, Lafage V, Schwab FJ, Protopsaltis T, Scheer JK, Mundis GM, Fu K-MG (2014) Prospective multicenter assessment of risk factors for rod fracture following surgery for adult spinal deformity. *J Neurosurg Spine* 21:994–1003
7. Kim YC, Kim KT, Kim CK, Hwang IY, Jin WY, Lenke LG, Cha JR (2019) Outcomes of non-operative management for Pseudarthrosis after pedicle subtraction osteotomies at minimum 5 years follow-up. *J Korean Neurosurg Soc* 62:567–576. <https://doi.org/10.3340/jkns.2018.0191>
8. Kim YJ, Bridwell KH, Lenke LG, Cheh G, Baldus C (2007) Results of lumbar pedicle subtraction osteotomies for fixed sagittal imbalance: a minimum 5-year follow-up study. *Spine* 32:2189–2197
9. Luca A, Lovi A, Galbusera F, Brayda-Bruno M (2014) Revision surgery after PSO failure with rod breakage: a comparison of different techniques. *Eur Spine J* 23:610–615
10. Hyun SJ, Lenke LG, Kim YC, Koester LA, Blanke KM (2014) Comparison of standard 2-rod constructs to multiple-rod constructs for fixation across 3-column spinal osteotomies. *Spine (Phila Pa 1976)* 39:1899–1904. <https://doi.org/10.1097/brs.0000000000000556>
11. La Barbera L, Wilke HJ, Ruspi ML, Palanca M, Liebsch C, Luca A, Brayda-Bruno M, Galbusera F, Cristofolini L (2021) Load-sharing biomechanics of lumbar fixation and fusion with pedicle subtraction osteotomy. *Sci Rep* 11:3595. <https://doi.org/10.1038/s41598-021-83251-8>
12. Luca A, Ottardi C, Sasso M, Prosdocimo L, La Barbera L, Brayda-Bruno M, Galbusera F, Villa T (2017) Instrumentation failure following pedicle subtraction osteotomy: the role of rod material, diameter, and multi-rod constructs. *Eur Spine J* 26:764–770. <https://doi.org/10.1007/s00586-016-4859-8>
13. Hallager DW, Gehrchen M, Dahl B, Harris JA, Gudipally M, Jenkins S, Wu AM, Bucklen BS (2016) Use of supplemental short pre-contoured accessory rods and cobalt chrome alloy posterior rods reduces primary rod strain and range of motion across the pedicle subtraction osteotomy level: an in vitro biomechanical study. *Spine (Phila Pa 1976)* 41:E388–395. <https://doi.org/10.1097/brs.0000000000001282>
14. La Barbera L, Brayda-Bruno M, Liebsch C, Villa T, Luca A, Galbusera F, Wilke HJ (2018) Biomechanical advantages of supplemental accessory and satellite rods with and without interbody cages implantation for the stabilization of pedicle subtraction osteotomy. *Eur Spine J* 27:2357–2366. <https://doi.org/10.1007/s00586-018-5623-z>
15. Seyed Vosoughi A, Joukar A, Kiapour A, Parajuli D, Agarwal AK, Goel VK, Zavatsky J (2019) Optimal satellite rod constructs to mitigate rod failure following pedicle subtraction osteotomy (PSO): a finite element study. *Spine J* 19:931–941. <https://doi.org/10.1016/j.spinee.2018.11.003>
16. Deviren V, Tang JA, Scheer JK, Buckley JM, Pekmezci M, McClellan RT, Ames CP (2012) Construct Rigidity after Fatigue Loading in Pedicle Subtraction Osteotomy with or without Adjacent Interbody Structural Cages. *Global Spine J* 2:213–220. <https://doi.org/10.1055/s-0032-1331460>
17. Jazini E, Gelb DE, Tareen J, Ludwig SC, Harris JA, Amin DB, Wang W, Van Horn MR, Patel PD, Mirabile BA, Bucklen BS (2021) Comprehensive in silico evaluation of accessory rod position, rod material and diameter, use of cross-connectors, and anterior column support in a pedicle subtraction osteotomy model: part II: effects on lumbosacral rod and screw strain. *Spine (Phila Pa 1976)* 46:E12–E22. <https://doi.org/10.1097/brs.0000000000003720>
18. El Dafrawy MH, Adogwa O, Wegner AM, Pallotta NA, Kelly MP, Kebaish KM, Bridwell KH, Gupta MC (2020) Comprehensive classification system for multirod constructs across three-column osteotomies: a reliability study. *J Neurosurg Spine* 34:103–109
19. Edwards WT, Zheng Y, Ferrara LA, Yuan HA (2001) Structural features and thickness of the vertebral cortex in the thoracolumbar spine. *Spine* 26:218–225
20. Momeni Shahrai N, Fatemi A, Goel VK, Agarwal A (2015) On the use of biaxial properties in modeling annulus as a Holzapfel–Gasser–Ogden material. *Front Bioeng Biotechnol* 3:69

21. Lindsey DP, Kiapour A, Yerby SA, Goel VK (2015) Sacroiliac joint fusion minimally affects adjacent lumbar segment motion: a finite element study. *Int J Spine Surg* 9:64
22. Wang H, Zhao Y, Mo Z, Han J, Chen Y, Yu H, Wang Q, Liu J, Li C, Zhou Y (2017) Comparison of short-segment monoaxial and polyaxial pedicle screw fixation combined with intermediate screws in traumatic thoracolumbar fractures: a finite element study and clinical radiographic review. *Clinics* 72:609–617
23. Hussein MA, Mohammed AS, Al-Aqeeli N (2015) Wear characteristics of metallic biomaterials: a review. *Materials* 8:2749–2768
24. Luca A, Ottardi C, Lovi A, Brayda-Bruno M, Villa T, Galbusera F (2017) Anterior support reduces the stresses on the posterior instrumentation after pedicle subtraction osteotomy: a finite-element study. *Eur Spine J* 26:450–456. <https://doi.org/10.1007/s00586-019-06087-x>
25. Berjano P, Xu M, Damilano M, Scholl T, Lamartina C, Jekir M, Galbusera F (2019) Supplementary delta-rod configurations provide superior stiffness and reduced rod stress compared to traditional multiple-rod configurations after pedicle subtraction osteotomy: a finite element study. *Eur Spine J* 28:2198–2207. <https://doi.org/10.1007/s00586-019-06012-2>
26. Scheer JK, Tang JA, Deviren V, Buckley JM, Pekmezci M, McClellan RT, Ames CP (2011) Biomechanical analysis of revision strategies for rod fracture in pedicle subtraction osteotomy. *Neurosurgery* 69:164–172
27. La Barbera L, Wilke HJ, Liebsch C, Villa T, Luca A, Galbusera F, Brayda-Bruno M (2020) Biomechanical in vitro comparison between anterior column realignment and pedicle subtraction osteotomy for severe sagittal imbalance correction. *Eur Spine J* 29:36–44. <https://doi.org/10.1007/s00586-019-06087-x>
28. Gelb DE, Tareen J, Jazini E, Ludwig SC, Harris JA, Amin DB, Wang W, Van Horn MR, Patel PD, Mirabile BA, Bucklen BS (2021) Comprehensive evaluation of accessory rod position, rod material and diameter, use of cross-connectors, and anterior column support in a pedicle subtraction osteotomy model: part I: effects on apical rod strain: an in vitro and in silico biomechanical study. *Spine (Phila Pa 1976)* 46:E1–E11. <https://doi.org/10.1097/brs.0000000000003723>

Publisher's Note Springer Nature remains neutral with regard to jurisdictional claims in published maps and institutional affiliations.